

Nuclear spin-lattice relaxation in ferromagnetic EuO

J. Barak, A. Gabai, and N. Kaplan

The Racah Institute of Physics, The Hebrew University of Jerusalem, Jerusalem, Israel

(Received 30 November 1973)

The spin-lattice relaxation time T_1 of Eu^{153} in powder EuO was measured at temperatures from 1.7 to 20 K and external fields above magnetic saturation from 24 to 60 kOe. The results were analyzed using the multimagnon scattering theory previously proposed by Beeman and Pincus. The observed relaxation rates are well explained by the dipolar-induced two-magnon process and exchange-scattering-enhanced three-magnon process. It is found that the first is dominant at low temperatures ($T < 14$ K) and the second at higher temperatures.

I. INTRODUCTION

In pure magnetic insulators, at temperatures which are low compared to the Curie or Néel temperatures, the excitations of spin waves through the hyperfine and the dipolar interactions between the nuclei and the electrons provide the main mechanism for nuclear spin-lattice relaxation. The contributions of the different processes with one or more magnons are obtained by expanding the electron spin operator \vec{S} of the above interactions in magnon-creating and -annihilating operators. The direct process which involves one magnon is usually not allowed by energy conservation. First calculations of the nuclear spin-lattice relaxation rates $1/T_1$ for the two-magnon process in antiferromagnets were made by Moriya¹ and by Van Kranendonk and Bloom², who found qualitative agreement between their theory and the experimental results of Hardman *et al.*³ on the protons in $\text{CuCl}_2 \cdot 2\text{H}_2\text{O}$. First calculations of the two-magnon mechanism for ferromagnets were presented by Mitchell⁴ and the three-magnon relaxation process was first considered by Oguchi and Keffer.⁵ Second-order mechanisms like the ferromagnetic exchange-scattering three-magnon process⁶ may enhance the first-order processes. Beeman and Pincus⁷ (BP) review the theory of the first-order processes, extend the theory of the exchange-scattering three-magnon process and develop the theory of the two-magnon process which is induced by the exchange interactions in canted antiferromagnets and by the electron magnetic dipole-dipole interaction in both ferromagnets and antiferromagnets.

In order to prevent relaxation through interactions with impurities in a quantitative experimental study of the intrinsic spin-lattice relaxation processes, one should have very pure samples. Successful application of the multimagnon scattering treatment in the study of T_1 in a pure insulating ferromagnet was made by Narath and Fromhold⁸ and in a pure antiferromagnet by Kaplan *et al.*⁹ In the first case, T_1 of Cr^{53} was measured in the ferromagnetic phase of CrCl_3 . The relaxation rate was attributed to the enhanced three-magnon pro-

cess. In the second case, T_1 of F^{19} in pure MnF_2 was measured and the results were well explained by the two-magnon process.

EuO was found to be a good system for further examination of the theory. It is nearly an ideal Heisenberg ferromagnet with comparatively high $T_c = 69.4$ K,¹⁰ which enables measurements at $T \ll T_c$ without undue difficulty. The structure of EuO is very simple (fcc NaCl type) and its thermodynamic and magnetic characteristics were widely studied. The first observations of T_1 of Eu^{153} in 97% pure EuO in zero external magnetic field and at 4.2 and 20.3 K, were made by Uriano and Streever.¹¹ They attributed the spin-echo signals to nuclei in domain walls and the relaxation mechanism to thermal fluctuations of these walls. Guenther *et al.*¹² extended these measurements in the range $1.2 \text{ K} \leq T \leq 4.2 \text{ K}$ and external magnetic fields $0 \leq H_0 \leq 14 \text{ kOe}$. They compare their results with Honma's theory,¹³ which was developed for ultra-low temperatures ($T < 0.15 \text{ K}$).

In our measurements we have studied T_1 of Eu^{153} in a powder sample of pure EuO in the range $1.7 \text{ K} \leq T \leq 20 \text{ K}$ and using external magnetic fields $24 \text{ kOe} \leq H_0 \leq 60 \text{ kOe}$. The excitations of the electronic system in the range $T \ll T_c$ are well described by noninteracting magnons¹⁴ and the magnetization M is not much different from the zero-temperature magnetization M_0 .¹⁵ The external magnetic fields were high enough ($H_0 \geq 4\pi M_0 = 24 \text{ kOe}$) to ensure that the sample contained single-domain particles. The experimental procedure and results are described in Sec. II. The relaxation rates due to two-magnon and three-magnon processes are calculated and compared with the experimental values in Sec. III. It is shown that the relaxations come from the dipolar-induced two-magnon process and the enhanced three-magnon process. The first process is dominant for $T < 14 \text{ K}$ and the second is dominant at the higher temperatures.

II. EXPERIMENTAL PROCEDURES AND RESULTS

The sample preparation and the spin-echo spectrometer system utilized are essentially similar

to those described in a recent paper.¹⁶ Because of the distribution of demagnetization fields caused by the distribution of shapes and directions of particles in the powder sample, the macroscopic linewidth is about $4\pi M/3$ (see Fig. 1). During preliminary measurements it was found that by using the method of a saturating comb of rf pulses followed by $\frac{1}{2}\pi-\pi$ pulses, a "hot spot" in the line was created. The recovery of the nuclear magnetization of this "hot spot" is caused by spin-lattice relaxation as well as by spin diffusion, resulting in a nonexponential echo recovery. In order to overcome this difficulty, most of the macroscopic line was simultaneously saturated by a long (100 msec) frequency-modulated high-power rf pulse transmitted by a sweep generator, followed by high-power amplifier connected to the sample coil through a Reed relay, to prevent noise at the time the echo appears. The nuclear magnetization was then sampled by a $\frac{1}{2}\pi-\pi$ echo at a time t after the modulated pulse. Exponential recovery $A(t) = A(\infty)(1 - e^{-t/T_1})$ was always observed by using this method.

$1/T_1$ was measured at the center of the macroscopic lines (see Fig. 1) for $1.7 \text{ K} \leq T \leq 20 \text{ K}$ and $24 \text{ kOe} \leq H_0 \leq 60 \text{ kOe}$. The effective anisotropy field H_a , acting on the Eu ions, is obtained¹⁶ by adding to H_0 the demagnetization field at the center of the macroscopic line, $-2\pi M$ (Fig. 1), the Lorentz local field $+4\pi M/3$ and the weak internal anisotropy field ($\sim -190 \text{ Oe}$).¹⁰ Thus $H_a \approx H_0 - 2\pi M/3 \approx H_0 - 4 \text{ kOe}$.

The temperature-dependent experimental $1/T_1$ is given in Fig. 2 for $H_a = 20, 29,$ and 56 kOe . The effective field dependence of the observed $1/T_1$ at 1.7, 2.2, 3, and 4.2 K is given in Fig. 3.

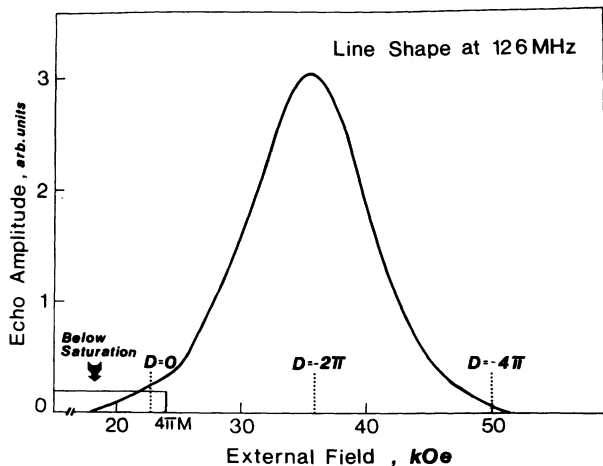


FIG. 1. Macroscopic spin-echo line profile of Eu^{153} in EuO at 126 MHz. The profile is nearly Gaussian with $2\sigma = 9 \text{ kOe}$.

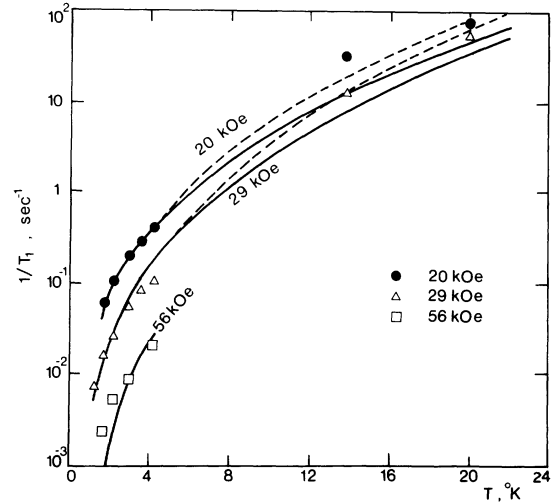


FIG. 2. Spin-lattice relaxation rates of Eu^{153} in powder EuO vs temperature for various external magnetic fields. The solid curves give the calculated $1/T_1$ for these fields, with an enhancement factor of 4 for the three-magnon process, and the dashed lines represent those calculated with an enhancement factor of 8.

III. CALCULATION OF RELAXATION RATES

A. Raman relaxation process

The processes which lead to nuclear spin-lattice relaxation in magnetic insulators were summarized by Beeman and Pincus.⁷ Following their theory, the direct process in which a single magnon is created while the nuclear spin is flipped is not allowed because of energy conservation; the change of energy due to the nuclear spin flip is much smaller than the minimum magnon energy $g\beta H_a$. Particularly in our experiments, where $H_a > 20 \text{ kOe}$, this process does not exist and the first process to be considered is the Raman relaxation process.

The Raman process involves two magnons. Assuming that the hyperfine interaction is isotropic, this relaxation process takes place only when there is an angle θ between the axes of quantization of the nuclear and electron spins. The relaxation rate is then proportional to $\sin^2\theta$.⁷ In an ideal ferromagnet, with a cubic structure, the resultant of the hyperfine field and the dipolar fields acting on the nucleus is parallel to the magnetization \vec{M} and one expects that $\theta = 0$. Quadrupolar interactions, however, may deviate the axis of the nuclear quantization from this direction. Charap and Bøyd¹⁷ observed a quadrupole splitting of Eu^{153} line in EuS . Very recently we found a similar splitting of the Eu^{153} line in preliminary studies of a spherical single crystal of EuO . The angular dependence of these lines shows an anisotropy which is equivalent to an anisotropy field of $H_{an} \approx 1 \text{ kOe}$, acting on the

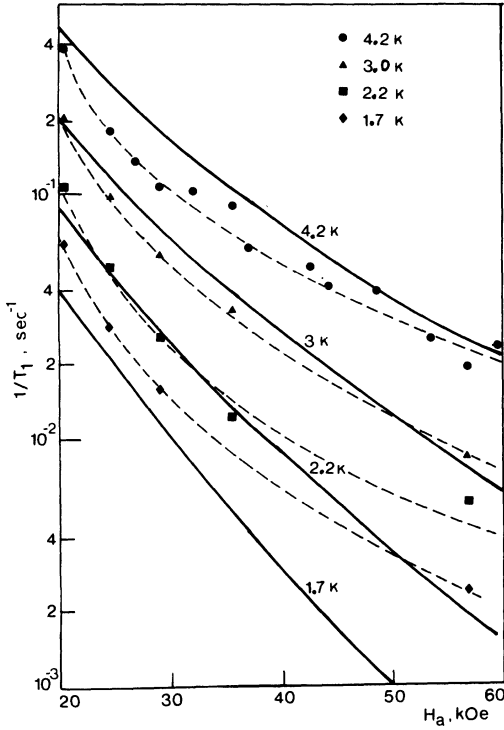


FIG. 3. Field-dependent spin-lattice relaxation rates of Eu^{153} in EuO for liquid-helium temperatures. The solid curves give the theoretical $1/T_1$ calculated for the dipolar-induced two-magnon process which is dominant at these conditions.

nuclei. The resultant magnetic field on the nuclei is $\vec{H}_t = \vec{H}_{\text{nr}} + \vec{H}_a + \vec{H}_{\text{nn}}$, where $H_{\text{nr}} = 303 \text{ kOe}^{16}$ is the hyperfine field. For H_t perpendicular to H_{nn} , θ may be estimated by $\theta \approx H_{\text{nn}}/H_t \approx 0.2^\circ$. Thus it is reasonable to take an upper limit of one degree for θ . This value will be used in the calculations. Following Beeman and Pincus (BP),⁷ the relaxation rate, induced by the Raman process, is given by

$$\frac{1}{T_1} = \frac{\pi}{\hbar} \left(\frac{A}{N} \right)^2 \sin^2 \theta \sum_{\vec{i}, \vec{i}'} n_{\vec{k}} (1 + n_{\vec{k}}) \delta(E_{\vec{k}} - E_{\vec{k}'}, -AS), \quad (1)$$

where $n_{\vec{k}} = (e^{E_{\vec{k}}/k_B T} - 1)^{-1}$, A is the hyperfine constant, and $E_{\vec{k}}$ is the energy of the spin waves for the wave vector \vec{k} . Charap and Boyd¹⁷ calculated $E_{\vec{k}}$ by first considering the exchange Hamiltonian

$$\mathcal{K}_{\text{ex}} = -2J_1 \sum_{\text{nn}} \vec{S}_i \cdot \vec{S}_j - 2J_2 \sum_{\text{nnn}} \vec{S}_i \cdot \vec{S}_j, \quad (2)$$

the summation being for $i < j$, where sites i and j are nearest neighbors (nn) or next-nearest neighbors (nnn). J_1 and J_2 are the corresponding exchange constants. This Hamiltonian leads to spin-wave energy given by

$$\epsilon_{\vec{k}} = 2SJ_1 \sum_{\vec{i}_1} (1 - e^{i\vec{k} \cdot \vec{i}_1}) + 2SJ_2 \sum_{\vec{i}_2} (1 - e^{i\vec{k} \cdot \vec{i}_2}), \quad (3)$$

where \vec{i}_1 denotes the displacement vectors to nn and \vec{i}_2 to nnn. When the dipolar interactions between the electron spins and the Zeeman energy in an external magnetic field are added to \mathcal{K}_{ex} , the spin-wave energy becomes¹⁷

$$E_{\vec{k}} = (\epsilon_{\vec{k}} + g\mu_B H) (1 + \phi_{\vec{k}} \sin^2 \theta_{\vec{k}})^{1/2}. \quad (4)$$

Here H is the sum of the anisotropic field, the demagnetization field, and the external field, $\theta_{\vec{k}}$ is the angle between \vec{k} and \vec{M} , and

$$\phi_{\vec{k}} = 4\pi g\mu_B M / (\epsilon_{\vec{k}} + g\mu_B H). \quad (5)$$

For $\phi_{\vec{k}} \ll 1$ (which is the case in the present experiments), $\sin^2 \theta_{\vec{k}}$ may be replaced by its average value $\frac{2}{3}$ to give¹⁷

$$E_{\vec{k}} = \epsilon_{\vec{k}} + g\mu_B H_a, \quad (6)$$

where $H_a = H + 4\pi M/3$ is the resultant field on the electron, considered in Sec. II and $4\pi M/3$ is the Lorentz local field.

Returning to Eq. (1) and replacing $(1/N) \sum_{\vec{k}} F(E_{\vec{k}})$, where $F(E_{\vec{k}})$ are the summed terms in (1), by $\int F(E) \nu(E) dE$, where $\nu(E)$ is the density of states of the spin waves, and assuming that $AS \ll g\mu_B H_a$, Eq. (1) becomes

$$\frac{1}{T_1} = \frac{\pi A^2 \sin^2 \theta}{\hbar} \iint \frac{e^{E'/k_B T}}{(e^{E'/k_B T} - 1)(e^{E/k_B T} - 1)} \times \delta(E - E') \nu(E) \nu(E') dE dE'. \quad (7)$$

The integration is over the interval where $\nu(E) \neq 0$. Defining $N(\epsilon)$ as the density of states for $H_a = 0$ gives $\nu(E) = N(E - g\mu_B H_a) = N(\epsilon)$ and (7) becomes

$$\frac{1}{T_1} = \frac{\pi A^2 \sin^2 \theta}{\hbar} \int \frac{e^{(\epsilon + g\mu_B H_a)/k_B T}}{(e^{(\epsilon + g\mu_B H_a)/k_B T} - 1)^2} N^2(\epsilon) d\epsilon. \quad (8)$$

The density-of-states spectra for fcc lattice with various values of J_2/J_1 were analyzed by Loly and Buchheit¹⁸ and by Swendsen and Callen.¹⁹ Because of disagreement among various groups concerning the appropriate values of J_1 , J_2 [Eqs. (2) and (3)], we have calculated $N(\epsilon)$ for two different sets of J_1, J_2 values. Using $J_1/k_B = 0.75 \text{ K}$, and $J_2/k_B = -0.0975 \text{ K}^{15,20}$ $N(\epsilon)$ is shown by the solid line in Fig. 4. Using $J_1/k_B = 0.53 \text{ K}$, and $J_2/J_1 = 0.5$,^{21,22} $N(\epsilon)$ is plotted in Fig. 4 as a dotted line. At low energies, which correspond to small k values, Eq. (3) may be approximated by

$$\epsilon_k = 2JSa^2 k^2, \quad (9)$$

where $J \equiv J_1 + J_2$ has similar values in both cases. The two $N(\epsilon)$ curves coincide here since, in addition to the same shape at low energies, the corresponding $\epsilon_{\vec{k}}$ have a similar energy range. Because of Bose-Einstein distributions in (8), the low energies give the principal part of the integral and it was found that the calculation of $1/T_1$ is insensitive to the difference between the two sets of

the exchange constants. The calculations also give the same $1/T_1$ when using Eq. (4), confirming the validity of the approximation (6).

The temperature-dependent $1/T_1$ curve, computed from (8) with $A = \hbar f_0/S$, where $f_0 = 141$ MHz,¹⁶ $\theta = 1^\circ$, $H_a = 29$ kOe, and $S = \frac{7}{2}$, is plotted in Fig. 5, where it is labeled "Raman relaxation process."

B. Three-magnon process

In this process the relaxation of the nuclear spin is accompanied by the destruction of a magnon and the creation of two magnons. The interaction producing this process is⁷

$$\mathcal{H}' = \frac{-A}{8SN} \left(\frac{2S}{N} \right)^{1/2} I^+ \sum_{\vec{k}_1, \vec{k}_2, \vec{k}_3} b_{\vec{k}_1}^\dagger b_{\vec{k}_2}^\dagger b_{\vec{k}_3}^\dagger, \quad (10)$$

which connects between an initial state $|i\rangle$ with a magnon \vec{k}_3 and a nuclear-spin quantum number m , and a final state $|f\rangle$ with magnons \vec{k}_1 and \vec{k}_2 and a nuclear-spin quantum number $m+1$. Following the method used by BP in deriving Eq. (1)⁷ we substitute \mathcal{H}' in Fermi's golden rule

$$W = \frac{2\pi}{\hbar} \sum_f |\langle f | \mathcal{H}' | i \rangle|^2 \delta(E_i - E_f), \quad (11)$$

where W is the transition probability, from which one deduces T_1 by using the relation²³

$$T_1 = [(I - m)(I + m + 1)] / 2W, \quad (12)$$

provided the spin system is initially at a well-defined spin temperature (see Sec. II).

With $\langle b_{\vec{k}}^\dagger b_{\vec{k}} \rangle = n_{\vec{k}}$, this gives

$$\frac{1}{T_1} = \frac{\pi A^2}{8\hbar SN^3} \sum_{\vec{k}_1, \vec{k}_2, \vec{k}_3} (1 + n_{\vec{k}_1})(1 + n_{\vec{k}_2}) n_{\vec{k}_3} \times \delta(E_{\vec{k}_3} - E_{\vec{k}_1} - E_{\vec{k}_2} - AS). \quad (13)$$

Substituting $\sum_{\vec{k}}$ with an integration over energy leads to

$$\frac{1}{T_1} = \frac{\pi A^2}{8\hbar S} \iint \frac{e^{(\epsilon_1 + g\mu_B H_a)/k_B T}}{e^{(\epsilon_1 + g\mu_B H_a)/k_B T} - 1} \times \frac{e^{(\epsilon_2 + g\mu_B H_a)/k_B T}}{e^{(\epsilon_2 + g\mu_B H_a)/k_B T} - 1} \frac{N(\epsilon_1)N(\epsilon_2)N(\epsilon_1 + \epsilon_2)}{e^{(\epsilon_1 + \epsilon_2 + 2g\mu_B H_a)/k_B T} - 1} \times d\epsilon_1 d\epsilon_2. \quad (14)$$

In addition to the above process, it has been pointed out previously⁶ that the fourth-order expansion of the ferromagnetic exchange interaction in magnon operators may scatter, by means of a thermal magnon, the virtual magnon being emitted when the nuclear spin is flipped in a *direct process*. The result is⁶ a second-order three-magnon process which enhances the first-order process. The enhancement factor for $g\mu_B H_a \ll k_B T$ and small- k approximation (9), was estimated by BP to be 8. In our case $g\mu_B H_a$ is of the order $k_B T$ and the process is field dependent. Freyne²⁴ has found that three-magnon relaxation rates calculated from (11) are enhanced by a factor of 4. The temperature dependence of this $1/T_1$ process, labeled "enhanced three-magnon process," is displayed in Fig. 5 for $H_a = 29$ kOe.

C. Dipolar-induced two-magnon process

Besides the influence of the dipolar interactions on the spin-wave spectrum, taken into account in Eq. (4), they may scatter via their $S_z S^+$ terms a virtual magnon created in the direct process. The net result is a second-order two-magnon process. For $H \gg M$, BP used the quadratic approximation (9) and obtained

$$\frac{1}{T_1} = \frac{A^2}{10\hbar JSn^2} \left(\frac{g\mu_B M}{2JS} \right)^2 \left(\frac{I_1}{3} \frac{k_B T}{g\mu_B H} + \frac{I_2}{4} \right), \quad (15)$$

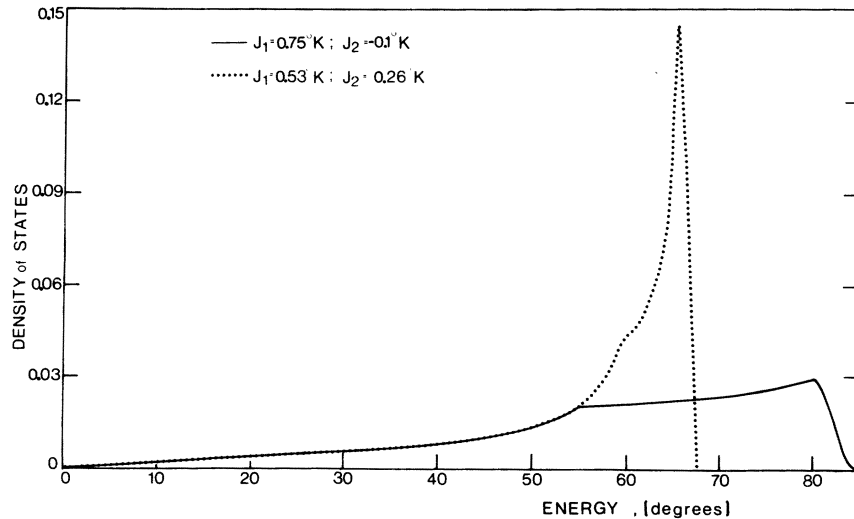


FIG. 4. Density of states $N(\epsilon)$ of spin waves in EuO for two suggested sets of J_1 and J_2 . The energy is given in units of degrees and both curves are normalized, $\int N(\epsilon) d\epsilon = 1$.

where n is the number of sites in the unit cell (four for fcc) and

$$I_1 = \int_{x_0}^{\infty} \frac{4x - 7x_0}{4x - 3x_0} \frac{e^x}{(e^x - 1)^2} dx \quad (16)$$

and

$$I_2 = \int_{x_0}^{\infty} \frac{dx}{x - x_0} \ln \left(\frac{4x - 3x_0}{x_0} \right) \frac{e^x}{(e^x - 1)^2}, \quad (17)$$

with $x_0 = g\mu_B H_a / k_B T$. The temperature dependence of $1/T_1$ due to this process, labeled "dipolar-induced two-magnon process," is given in Fig. 5 for $H_a = 29$ kOe.

D. Comparison with experiments

The sum of the relaxation rates of the various processes is plotted as a heavy solid line in Fig. 5. The dipolar-induced two-magnon process is shown to be dominant at low temperatures, while the enhanced three-magnon process is dominant at higher temperatures. The first-order two-magnon process is negligible throughout the whole range. This behavior is similar to BP calculations for Fe^{57} in YIG.⁷ The summed $1/T_1$ values for $H_a = 20, 29,$ and 56 kOe are plotted as solid curves in Fig. 2. These theoretical curves, which were computed without any adjustable parameter, are in reasonable agreement with the experimental results over more than four orders of magnitude. A better agreement is obtained if one assumes an enhancement factor of 8 for the three-magnon process (see

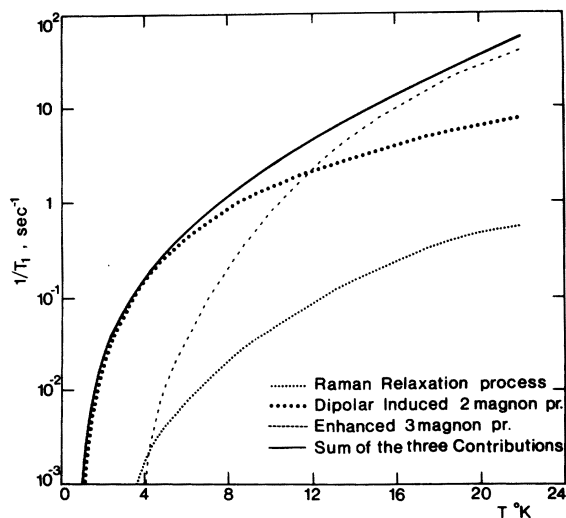


FIG. 5. Contributions to the temperature-dependent $1/T_1$ of Eu^{153} in EuO at 29 kOe, calculated for the two-magnon process with $\theta = 1^\circ$, the dipolar-induced two-magnon process, and the enhanced three-magnon process with an enhancement factor of 4. The sum of these relaxation rates is displayed by the heavy solid curve.

discussion in Sec. III B), as is shown by the dashed curves in Fig. 2.

The calculated field-dependent $1/T_1$ at liquid-helium temperatures are compared with the observed values in Fig. 3. Intrinsic mechanisms other than the dipolar-induced two-magnon process are of no significance at these temperatures. For low fields the agreement is good, while at high fields this process predicts $1/T_1$ smaller than observed.

IV. DISCUSSION AND CONCLUSIONS

The theory of Beeman and Pincus was found to give a good description of the spin-lattice relaxation in a Heisenberg ferromagnet. At temperatures $T > 14$ K the dominant mechanism for the relaxation is the enhanced three-magnon process. Calculations of $1/T_1$ due to this process were carried out by exact numeric integrations using the density-of-states spectrum. The enhancement factor, however, was calculated with the small- k approximation (9). This may account for the small difference between calculated and observed results at these temperatures. The expression (15) for the dipolar-induced two-magnon process is also based on this small- k approximation, leading to E_{\mp} higher than the exact value (6) and giving rise to lower relaxation rates, particularly for high magnetic fields. This might explain part of the discrepancy between theory and experiments at low temperatures and high fields (Fig. 2). The discrepancy may be further explained by interactions with impurities and free electrons which may exist, in small concentration, even in the stoichiometric sample.²⁵ These interactions might dominate at these extreme conditions (low T and high H_0), where $1/T_1$ is small.

The experimental results of Guenther *et al.*¹² which were found at liquid-helium temperatures, may also be explained by the dipolar-induced two-magnon process. As noted by BP, for $k_B T \ll g\mu_B H_a$, $1/T_1$ is proportional to $(T/H_a)^2$. This is in agreement with the temperature dependence of the observed T_1 for $H_0 = 0$, where the main contribution to the echo comes from the domain walls. In the walls the external and the demagnetization fields are screened and H_a is composed only of the local Lorentz field.¹⁶ $H_a = 2.6$ kOe is in best fit with these results. This value is to be compared with 4.1 kOe, found for the local Lorentz field in domain walls¹⁶ by comparing the resonance frequency of Eu^{153} in EuO above saturation $H_0 > 4\pi M$ and the zero-field frequency. When $H_0 > 0$ the signal of the walls is reduced and a greater part of the echo comes from the domains where H_a is different and may be smaller than in the walls, giving rise to greater $1/T_1$. This may explain the behavior of the observed $1/T_1$ vs H_0 ,¹⁶ where there is a mini-

mum at $H_0 = 6$ kOe, indicating that above this field the signal is mainly from the domains.

ACKNOWLEDGMENTS

We wish to thank I. B. Goldberg for his valuable

programming assistance. One of us (N. K.) wishes to acknowledge valuable discussions with A. Brooks Harris. In particular, it was A. Brooks Harris who pointed out to us the importance of the dipolar-induced two-magnon process in the present case of EuO.

-
- ¹T. Moriya, *Progr. Theor. Phys.* **16**, 23 (1956); *Prog. Theor. Phys.* **16**, 641 (1956).
- ²J. Van Kranendonk and M. Bloom, *Physica (Utr.)* **22**, 545 (1956).
- ³G. E. G. Hardman, N. J. Poulis, and W. van der Lugt, *Physica (Utr.)* **22**, 48 (1956).
- ⁴A. H. Mitchell, *J. Chem. Phys.* **27**, 17 (1957).
- ⁵T. Oguchi and F. Keffer, *J. Phys. Chem. Solids* **25**, 405 (1964).
- ⁶P. Pincus, *Phys. Rev. Lett.* **16**, 398 (1966).
- ⁷D. Beeman and P. Pincus, *Phys. Rev.* **166**, 359 (1968).
- ⁸A. Narath and A. T. Fromhold, *Phys. Rev. Lett.* **17**, 354 (1966).
- ⁹N. Kaplan, R. Loudon, V. Jaccarino, H. Guggenheim, D. Beeman, and P. A. Pincus, *Phys. Rev. Lett.* **17**, 357 (1966).
- ¹⁰S. Methfessel and D. C. Mattis, in *Handbüch der Physik*, edited by H. P. J. Wijn (Springer, New York, 1968), Vol. **18**, Pt. 1, p. 389.
- ¹¹G. A. Urriano and R. L. Streever, *Phys. Lett.* **17**, 205 (1965).
- ¹²B. D. Guenther, C. R. Christensen, A. C. Daniel, and D. T. Teaney, *J. Appl. Phys.* **40**, 1404 (1969).
- ¹³A. Honma, *Phys. Rev.* **142**, 306 (1966).
- ¹⁴F. Keffer, in *Handbüch der Physik*, edited by S. Flügge (Springer-Verlag, Berlin, 1966), Vol. **18**, Pt. 2.
- ¹⁵E. L. Boyd, *Phys. Rev.* **145**, 174 (1966).
- ¹⁶J. Barak, I. Siegelstein, A. Gabai, and N. Kaplan, *Phys. Rev. B* **8**, 5282 (1973).
- ¹⁷S. H. Charap and E. L. Boyd, *Phys. Rev.* **133**, A811 (1964).
- ¹⁸P. D. Loly and M. Buchheit, *Phys. Rev. B* **5**, 1986 (1972).
- ¹⁹R. H. Swendsen and H. Callen, *Phys. Rev. B* **6**, 2860 (1972).
- ²⁰A. J. Henderson, G. R. Brown, T. B. Reed, and H. Meyer, *J. Appl. Phys.* **41**, 946 (1970).
- ²¹N. Menyuk, K. Dwight, and T. B. Reed, *Phys. Rev. B* **3**, 1689 (1971).
- ²²R. H. Swendsen, *Phys. Rev. B* **5**, 116 (1972).
- ²³N. Blombergen, E. M. Purcell, and R. V. Pound, *Phys. Rev.* **73**, 679 (1948).
- ²⁴F. Freyne (private communication).
- ²⁵M. W. Shafer, J. B. Torrance, and D. Penney, *AIP Conf. Proc.* **5**, 840 (1972).